Science Advances
AAAS

Supplementary Materials for

Time-evolved hetero-alkali interphases enable long-life sulfide-based anode-free solid-state batteries

Jiwei Wang *et al.*

Corresponding author: Hongli Zhu, h.zhu@neu.edu

Sci. Adv. **12**, eael0210 (2026)
DOI: 10.1126/sciadv.ael0210

This PDF file includes:

Figs. S1 to S26

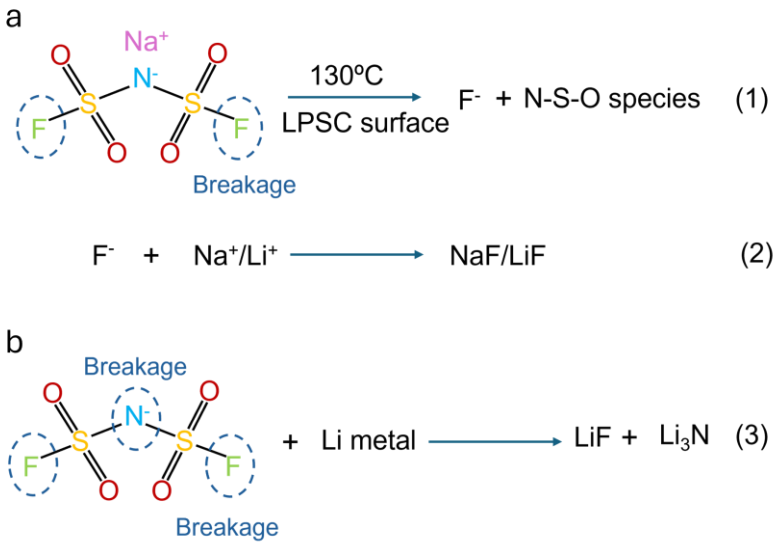


Figure S1. Proposed reaction pathways for the stepwise formation of the hetero-alkali interphase. (a) Chemical reaction process before cycle. (b) Electrochemical reaction process during cycle.

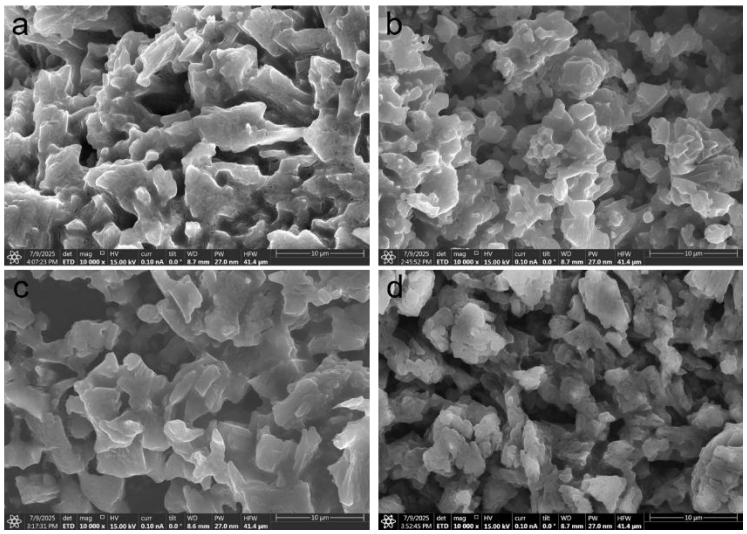


Figure S2. Surface morphology of NaFSI-modified LPSC. SEM images of the (a) bare LPSC, (b) 3NF@LPSC, (c) 5NF@LPSC, and (d) 7NF@LPSC.

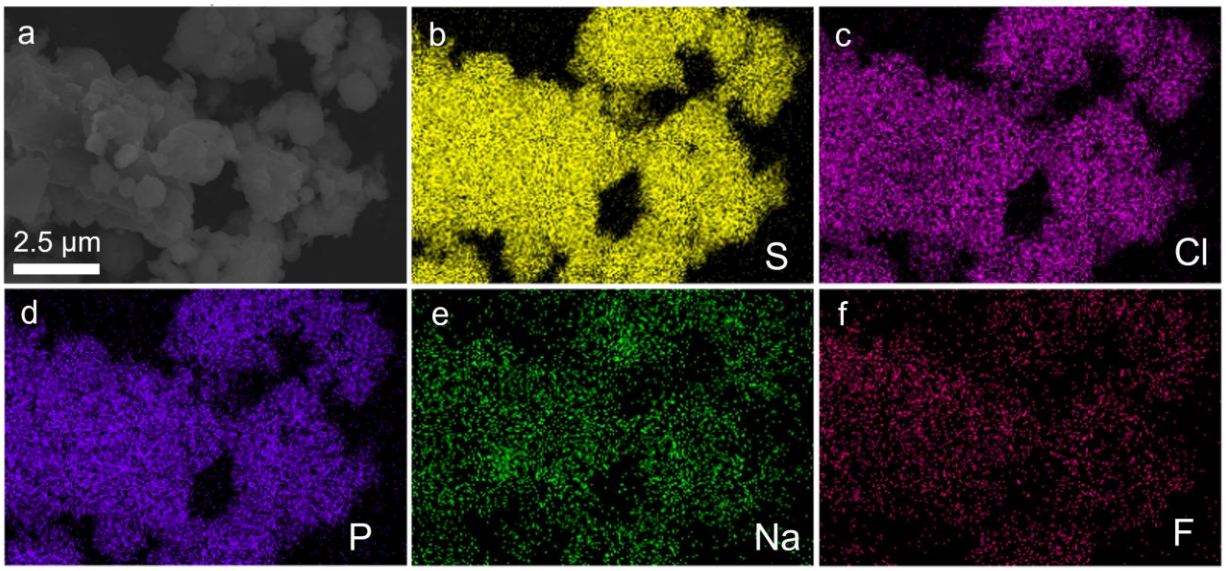


Figure S3. **Morphology and elemental distribution of 5NF@LPSC**. (a) SEM image and (b-f) the corresponding EDS mapping of 5NF@LPSC.

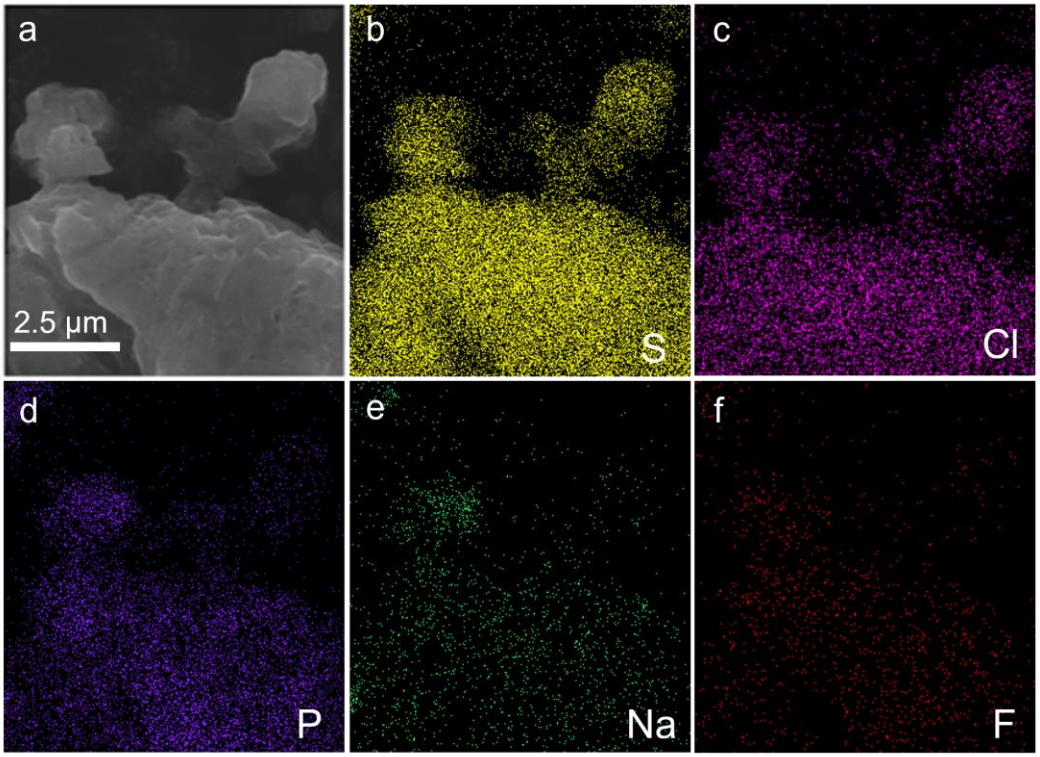


Figure S4. **Morphology and elemental distribution of 7NF@LPSC**. (a) SEM image and (b-f) the corresponding EDS mapping of 7NF@LPSC.

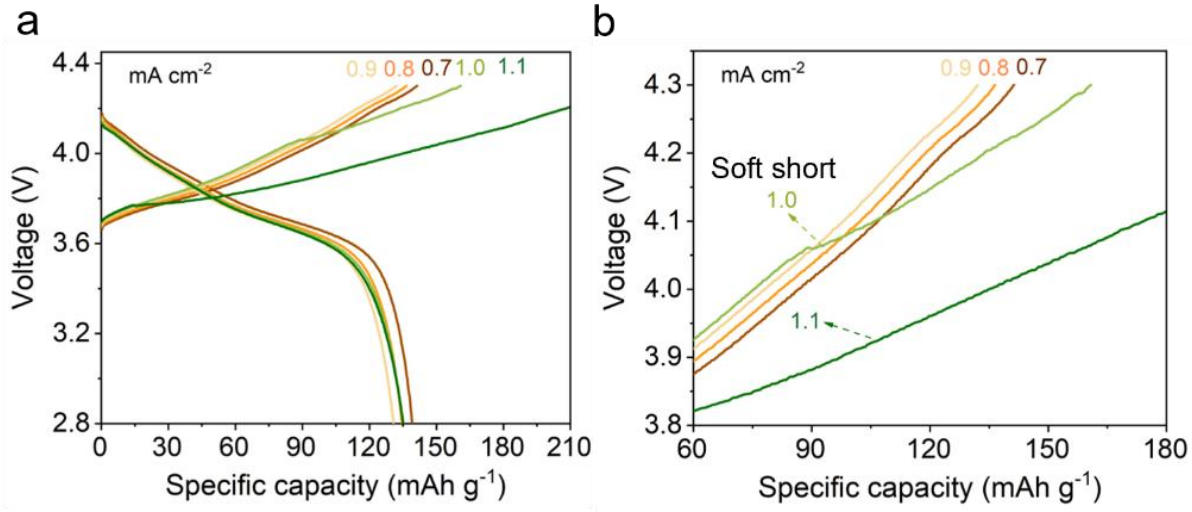


Figure S5. Soft-short behavior of AFSSBs with bare LPSC at high current densities. (a) Voltage profiles of AFSSB with bare LPSC SE cycled at current densities from 0.7 to 1.1 mA cm^{-2}. (b) Enlarged charge profiles showing the soft short occurring at 1.0 mA cm^{-2}.

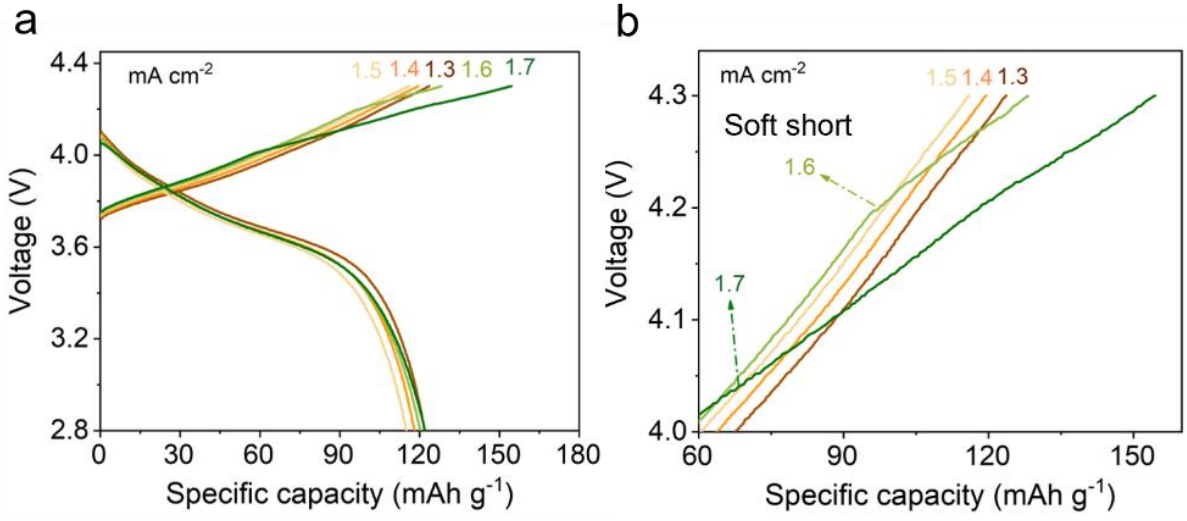


Figure S6. Soft-short behavior of the AFSSB with the 3NF@LPSC interlayer. (a) Voltage profiles of AFSSB with 3NF@LPSC interlayer cycled at current densities from 1.3 to 1.7 mA cm^{-2}. (b) Enlarged charge profiles showing the soft short occurring at 1.6 mA cm^{-2}.

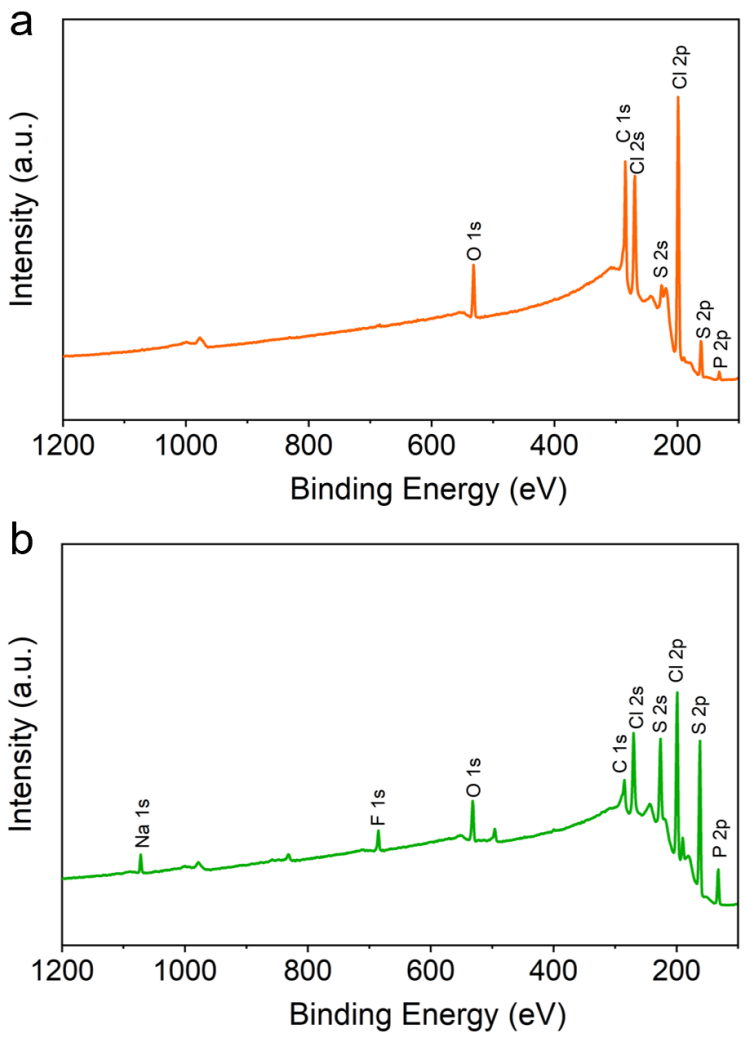


Figure S7. XPS survey spectra before cycling. (a) LPSC and (b) 3NF@LPSC.

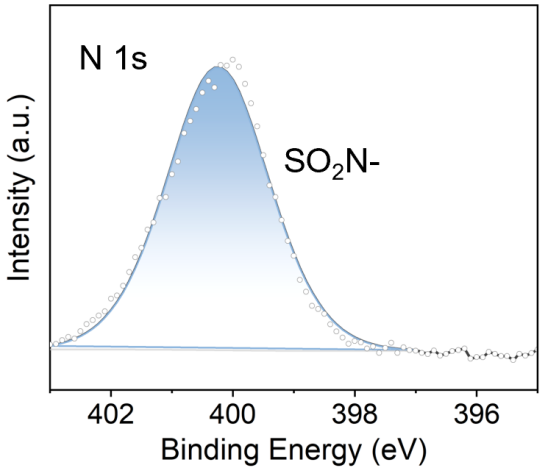


Figure S8. N 1s XPS spectrum of the pure NaFSI.

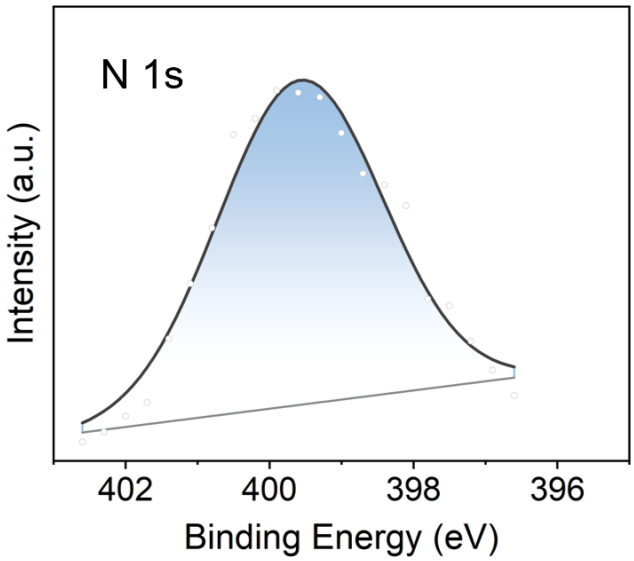


Figure S9. N 1s XPS spectrum of the 3NF@LPSC before cycle.

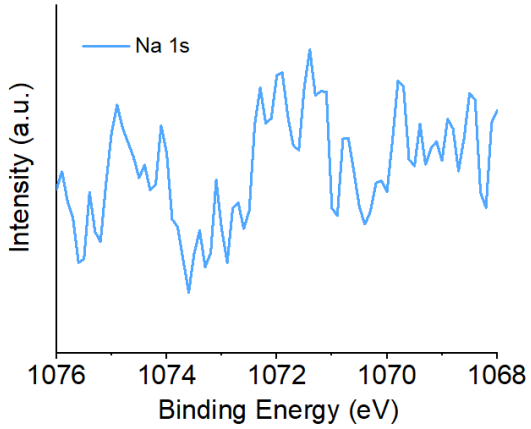


Figure S10. Na 1s XPS spectrum of cycled 3NF@LPSC

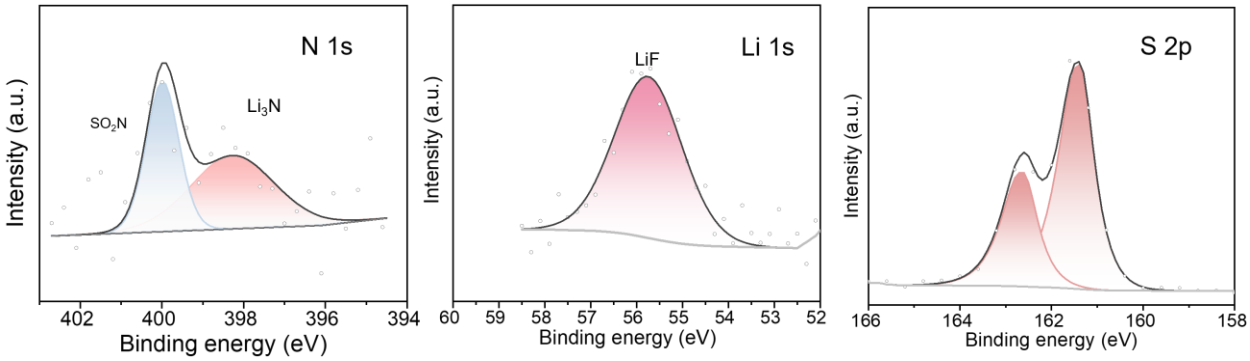


Figure S11. N 1s, Li 1s, and S 2p spectra of the 3NF@LPSC after one cycle.

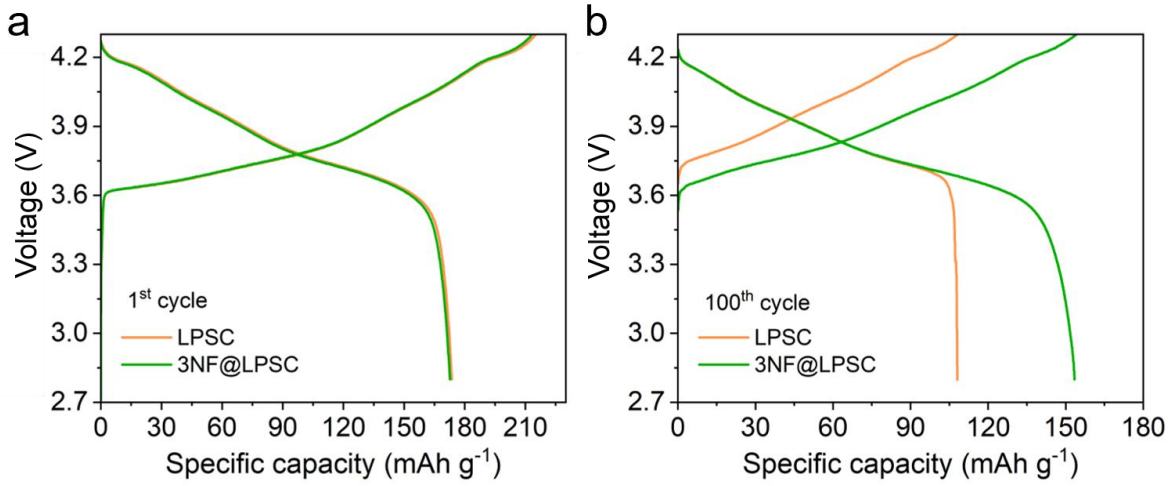


Figure S12. Charge-discharge voltage profiles of AFSSBs with and without 3NF@LPSC interlayer at 0.1 C. (a) 1st cycle and (b) 100th cycle.

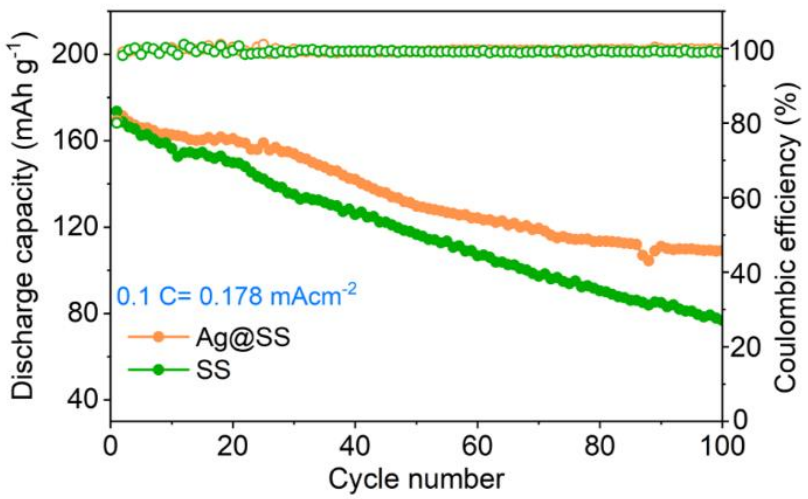


Figure S13. Cycling performance comparison of AFSSBs with Ag coated SS and bare SS current collectors

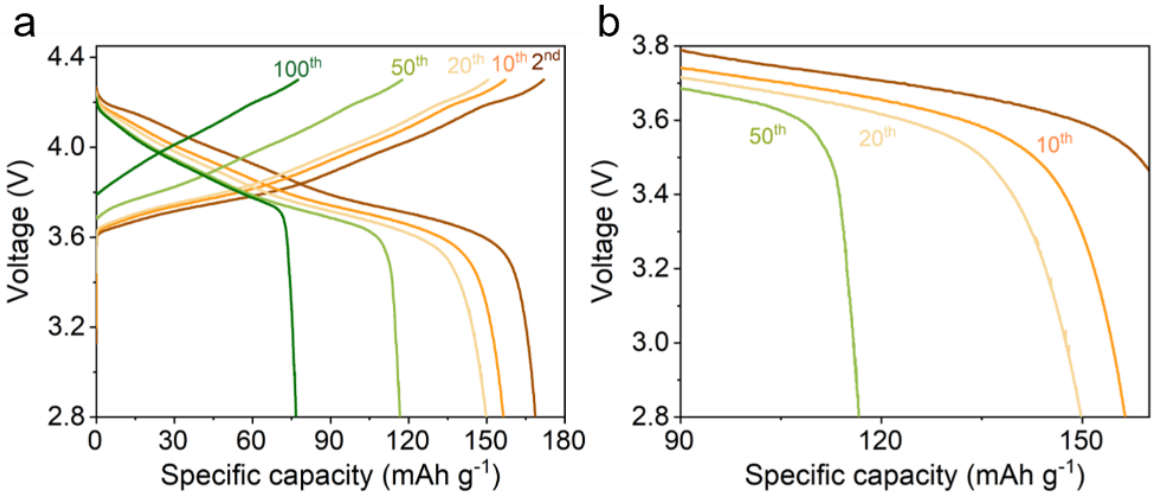


Figure S14. Voltage fluctuations of the AFSSB with bare LPSC during Li stripping. (a) Charge-discharge voltage profiles of AFSSB with bare LPSC SE and SS current collector at different cycles; (b) Detailed information showing the voltage fluctuation near the end of stripping process from 20th cycle.

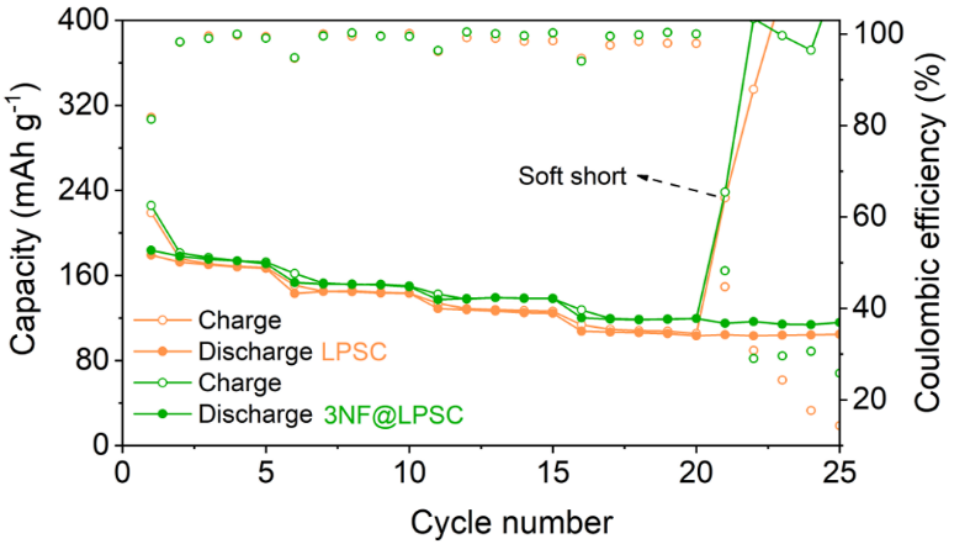


Figure S15. Rate capabilities of the AFSSBs with and without 3NF@LPSC.

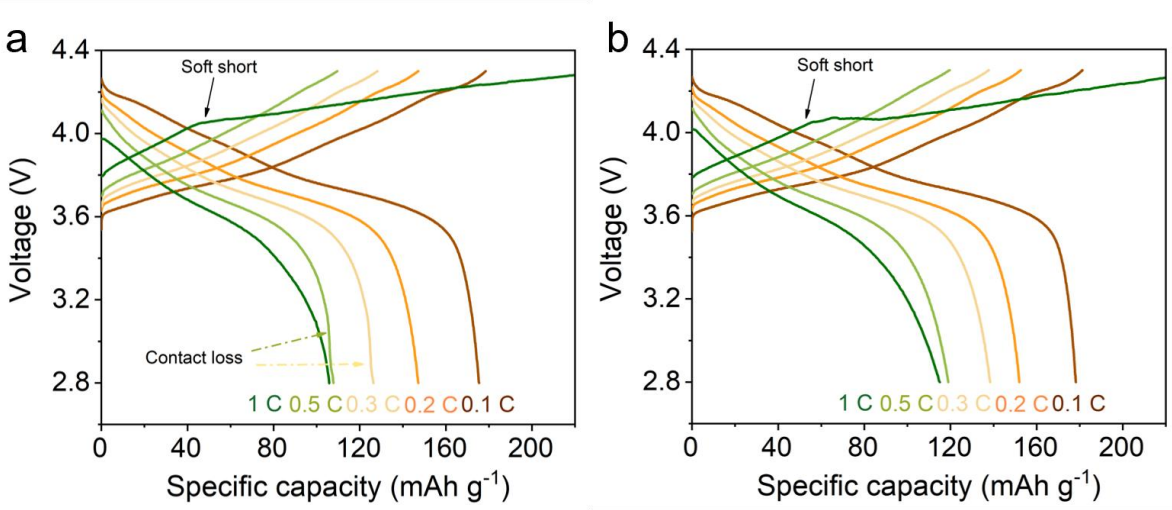


Figure S16. Rate-dependent charge-discharge behavior of AFSSBs with and without the 3NF@LPSC interlayer. Galvanostatic charge-discharge profiles of AFSSBs (a) without and (b) with the 3NF@LPSC interlayer at different rate.

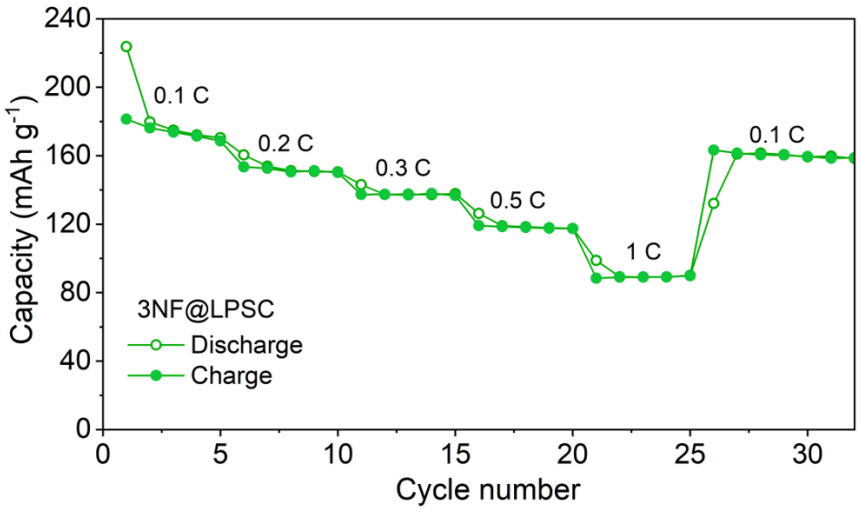


Figure S17. Rate capability of the cell with 3NF@LPSC interlayer using an active material mass loading of 6.24 mg cm^{-2}.

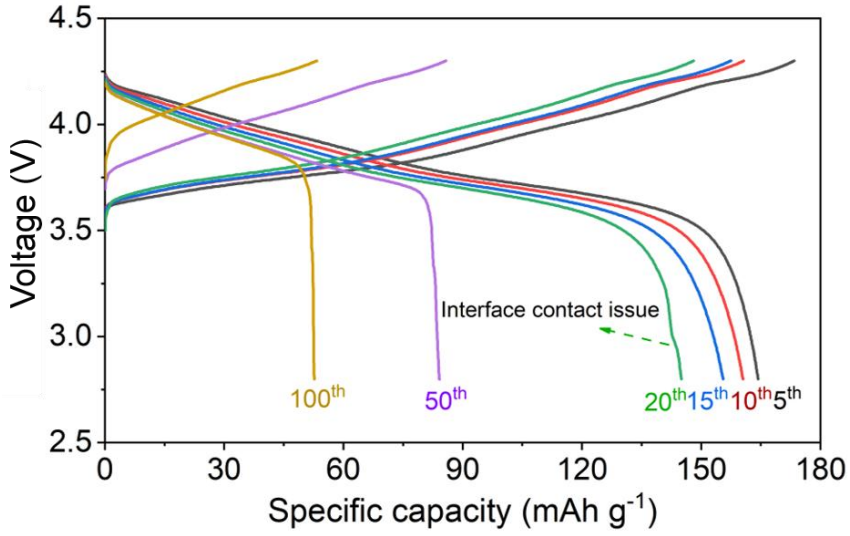


Figure S18. Galvanostatic charge/discharge profiles of AFSSBs without 3NF@LPSC interlayer cycled at 0.2 C at different cycles.

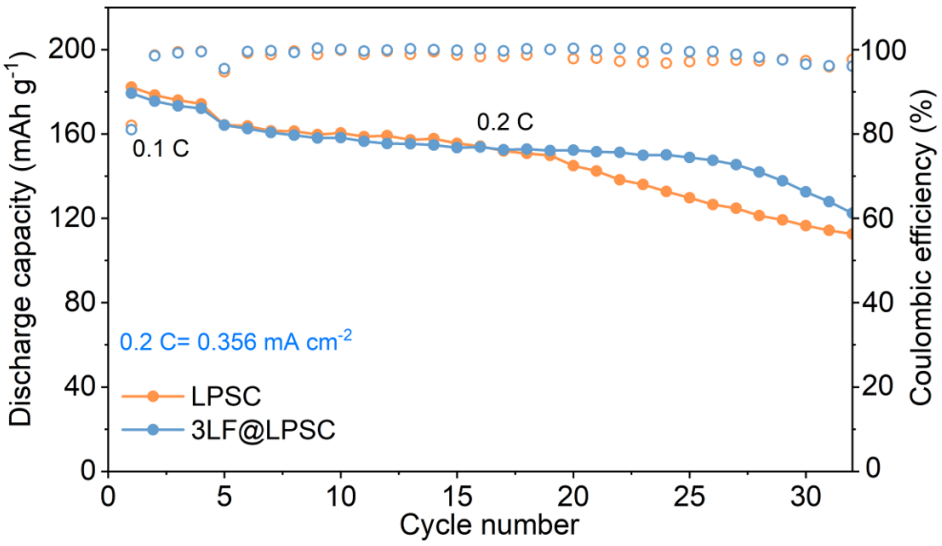


Figure S19. Cycling performance of AFSSBs with 3LiFSI@LPSC (3LF@LPSC) interlayer at 0.2 C (NMC loading: 8.92 mg cm^{-2}).

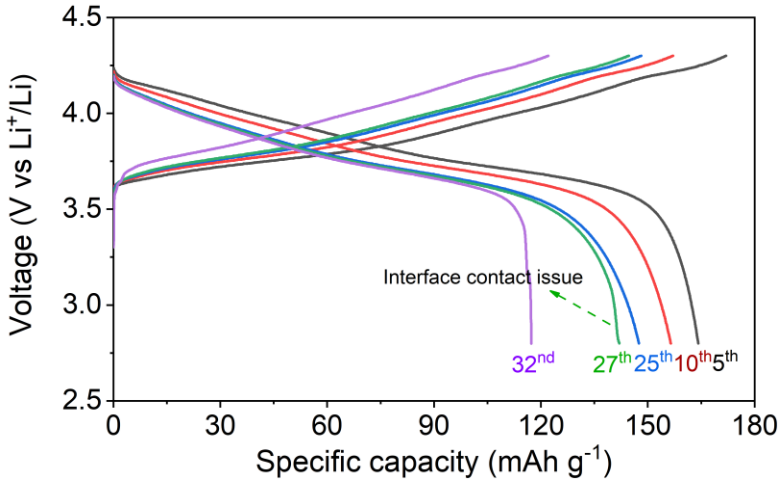


Figure S20. Galvanostatic charge-discharge profiles of AFSSBs with 3LF@LPSC interlayer cycled at 0.2 C at different cycles.

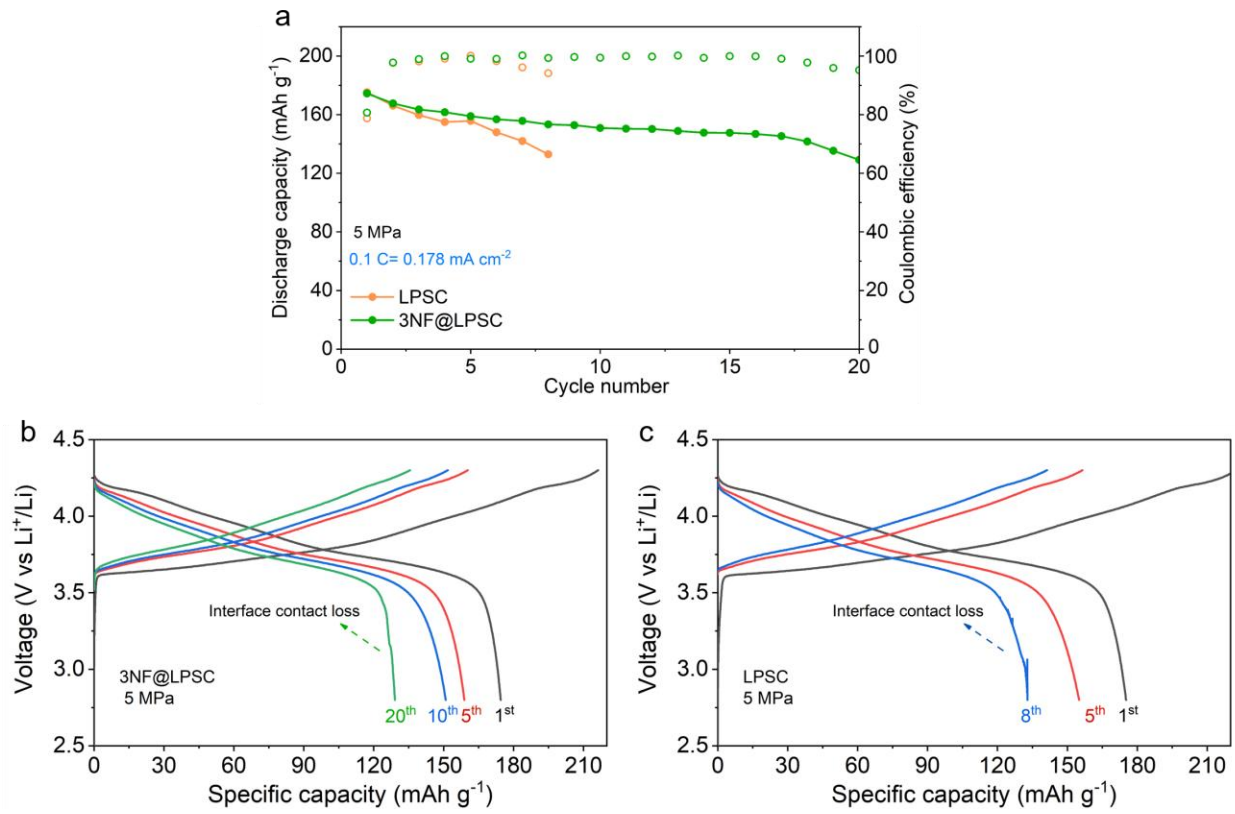


Figure S21. **Cycling performance of AFSSBs with the 3NF@LPSC interlayer under low stack pressure.** (a) Cycling performance of AFSSBs with and without 3NF@LPSC interlayer at 0.1 C (NMC loading: 8.92 mg cm^{-2}) with a stack pressure of 5 MPa. (b) and (c) Corresponding galvanostatic charge/discharge profiles of AFSSBs with and without 3NF@LPSC interlayer.

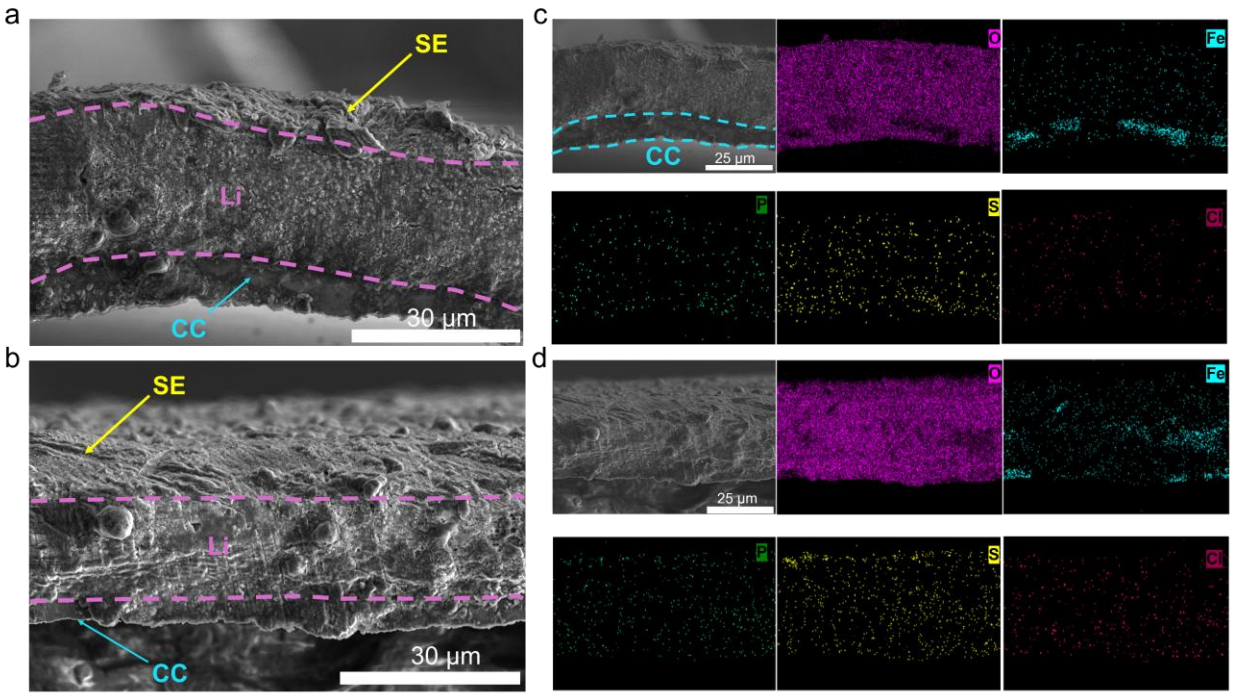


Figure S22. Morphology of deposited Li with and without the 3NF@LPSC interlayer. Cross-sectional SEM images of the deposited Li in the cells without (a) and with (b) 3NF@LPSC interlayer after 5 cycles at 0.1 C. (c) and (d) are the corresponding EDX mapping images.

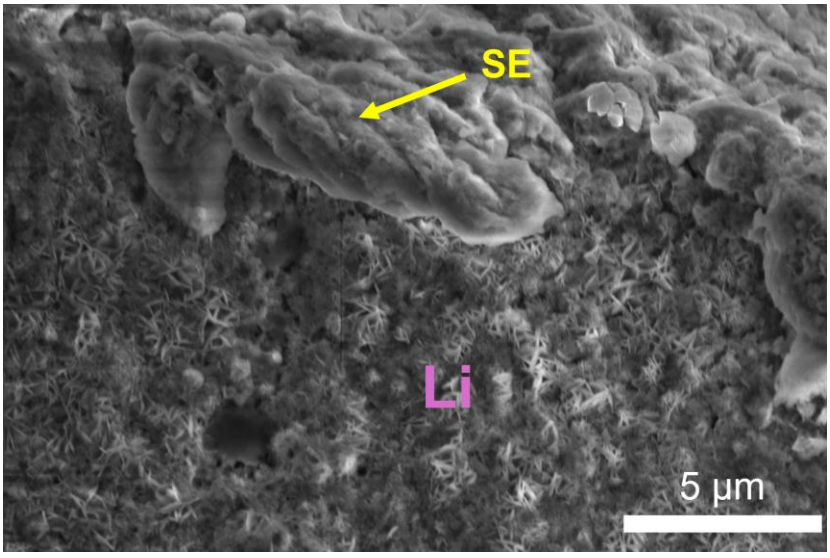


Figure S23. Enlarged cross-sectional SEM images of the deposited Li in Figure S22a.

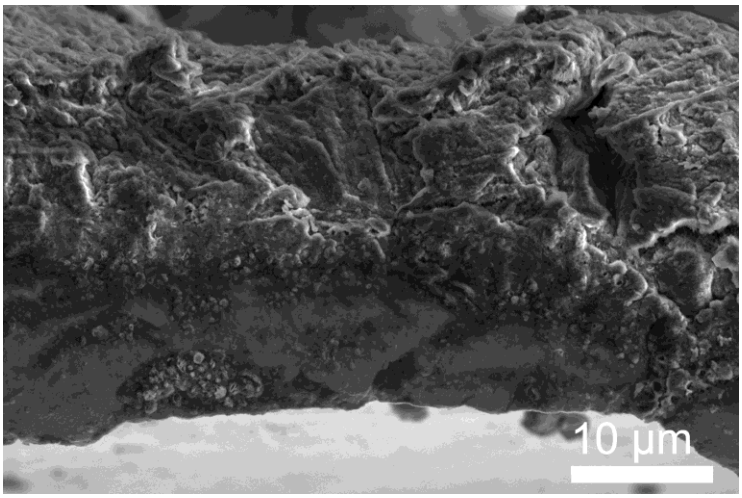


Figure S24. Cross-sectional morphology of deposited Li without the 3NF@LPSC interlayer. Another location of the cross-sectional SEM images of the deposited Li in the cells without 3NF@LPSC interlayer after 5 cycles at 0.1 C. Showing much lower Li thickness than that in Figure S22a.

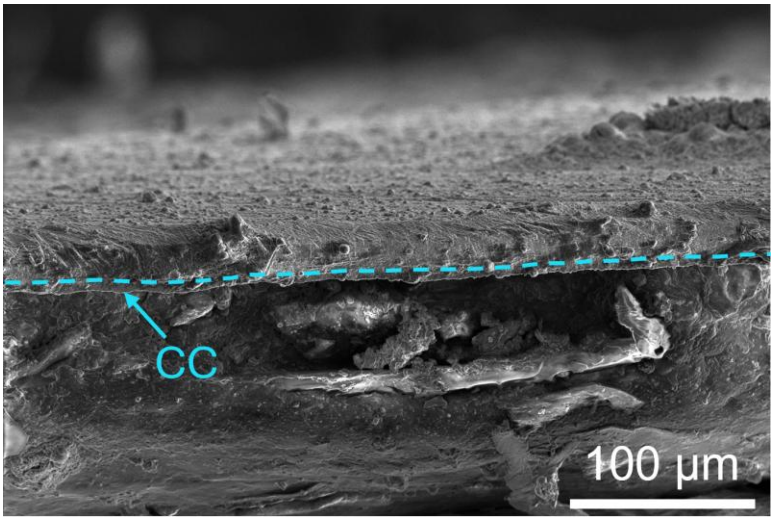


Figure S25. Cross-sectional morphology of deposited Li with the 3NF@LPSC interlayer. Low magnification of cross-sectional SEM images of the deposited Li in the cells with 3NF@LPSC interlayer after 5 cycles at 0.1 C.

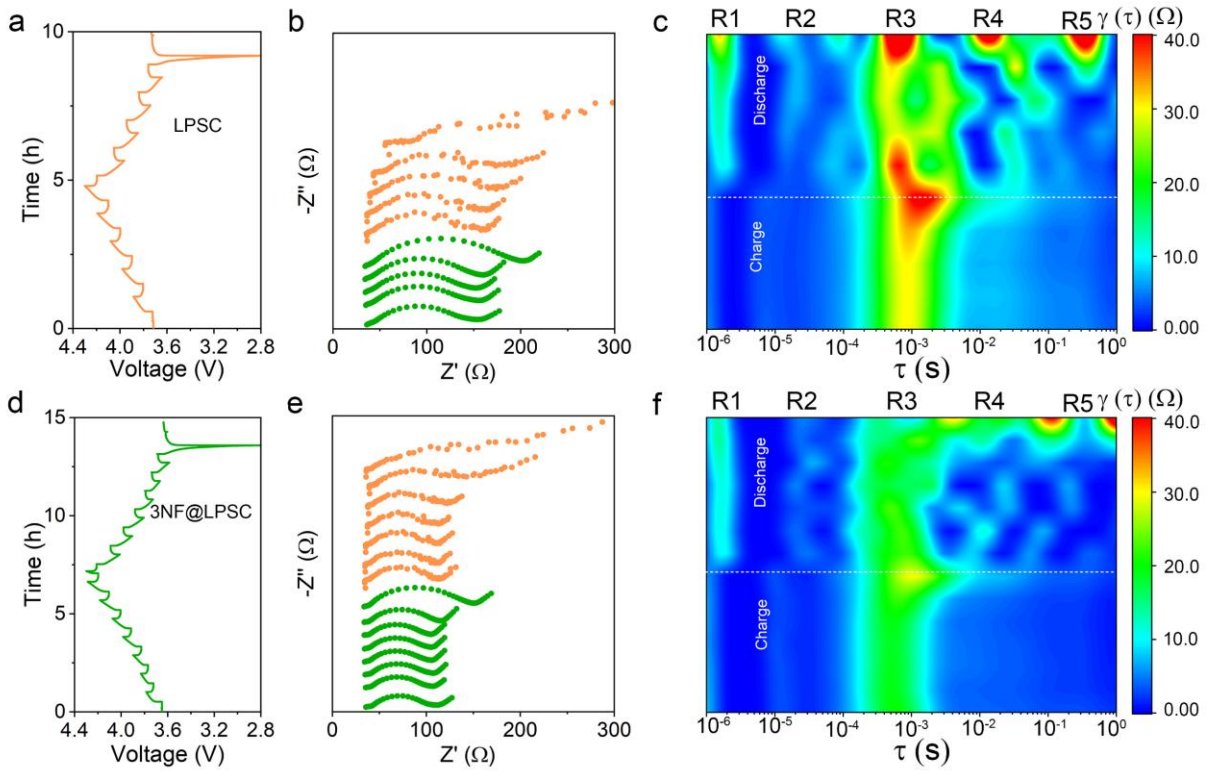


Figure S26. Interfacial resistance of AFSSBs during the 20th cycle revealed by in situ EIS and DRT. Charge-discharge profiles cells (a) without and (d) with 3NF@LPSC interlayer at 20th cycles in the EIS measurements. In situ EIS plots of cells (b) without and (e) with 3NF@LPSC interlayer. DRT contour plots of cells (c) without and (f) with 3NF@LPSC interlayer.